

Acclimation of Foliar Respiration and Photosynthesis in Response to Experimental Warming in a Temperate Steppe in Northern China

Yonggang Chi^{1,2}, Ming Xu^{1,3*}, Ruichang Shen^{1,2}, Qingpeng Yang^{1,4}, Bingru Huang⁵, Shiqiang Wan⁶

1 Key Laboratory of Ecosystem Network Observation and Modeling, Institute of Geographic Sciences and Natural Resources Research, Chinese Academy of Sciences, Beijing, China, **2** University of Chinese Academy of Sciences, Beijing, China, **3** Department of Ecology, Evolution and Natural Resources, Center for Remote Sensing and Spatial Analysis, Rutgers University, New Brunswick, New Jersey, United States of America, **4** Huitong Experimental Station of Forest Ecology, State Key Laboratory of Forest and Soil Ecology, Institute of Applied Ecology, Chinese Academy of Sciences, Shenyang, China, **5** Department of Plant Biology and Pathology, Rutgers University, New Brunswick, New Jersey, United States of America, **6** Key Laboratory of Plant Stress Biology, College of Life Sciences, Henan University, Kaifeng, Henan, China

Abstract

Background: Thermal acclimation of foliar respiration and photosynthesis is critical for projection of changes in carbon exchange of terrestrial ecosystems under global warming.

Methodology/Principal Findings: A field manipulative experiment was conducted to elevate foliar temperature (T_{leaf}) by 2.07°C in a temperate steppe in northern China. R_d/T_{leaf} curves (responses of dark respiration to T_{leaf}), A_n/T_{leaf} curves (responses of light-saturated net CO₂ assimilation rates to T_{leaf}), responses of biochemical limitations and diffusion limitations in gross CO₂ assimilation rates (A_g) to T_{leaf} , and foliar nitrogen (N) concentration in *Stipa krylovii* Roshev. were measured in 2010 (a dry year) and 2011 (a wet year). Significant thermal acclimation of R_d to 6-year experimental warming was found. However, A_n had a limited ability to acclimate to a warmer climate regime. Thermal acclimation of R_d was associated with not only the direct effects of warming, but also the changes in foliar N concentration induced by warming.

Conclusions/Significance: Warming decreased the temperature sensitivity (Q_{10}) of the response of R_d/A_g ratio to T_{leaf} . Our findings may have important implications for improving ecosystem models in simulating carbon cycles and advancing understanding on the interactions between climate change and ecosystem functions.

Citation: Chi Y, Xu M, Shen R, Yang Q, Huang B, et al. (2013) Acclimation of Foliar Respiration and Photosynthesis in Response to Experimental Warming in a Temperate Steppe in Northern China. PLoS ONE 8(2): e56482. doi:10.1371/journal.pone.0056482

Editor: Gil Bohrer, The Ohio State University, United States of America

Received: July 26, 2012; **Accepted:** January 14, 2013; **Published:** February 15, 2013

Copyright: © 2013 Chi et al. This is an open-access article distributed under the terms of the Creative Commons Attribution License, which permits unrestricted use, distribution, and reproduction in any medium, provided the original author and source are credited.

Funding: Financial support came from the National Key Research and Development Program of China (2010CB833500, <http://www.973.gov.cn>), the 100 Talents Program of the Chinese Academy of Sciences supported M. Xu's work (<http://www.cas.cn>) and National Natural Science Foundation (30925009, <http://www.nsf.gov.cn>). The funders had no role in study design, data collection and analysis, decision to publish, or preparation of the manuscript.

Competing Interests: The authors have declared that no competing interests exist.

* E-mail: mingxu@igsnr.ac.cn

Introduction

The balance between respiration and photosynthesis is critical to the exchange of carbon between the atmosphere and the terrestrial biosphere [1–3]. Instantaneous increases in foliar temperature (T_{leaf}) typically result in an increase in respiration/photosynthesis (R/A) ratio because the response of respiration to T_{leaf} normally follows an approximate exponential-type curve (at moderate temperatures) while the response of photosynthesis to T_{leaf} often bears a bell-shaped curve [i.e. the thermal optimum (T_{opt}) of respiration is higher than that of photosynthesis] [4,5]. In contrast, long-term warming experiments have suggested that R/A ratio is often conservative to changes in growth temperature (T_{growth}) through acclimation, the metabolic adjustment for compensating changes in T_{growth} [6–8]. Acclimation could occur via suppression of respiration in response to changes in foliar carbohydrate supplies [4,9]. The thermal acclimation of respiration and photosynthesis is associated with multitudes of signal cascades and networks, which involves the reallocation of resources to achieve and maintain not only optimal R/A ratio

but also protective strategies under sustained warming as projected by global climate models [10–12]. However, the mechanisms of thermal acclimation of respiration and photosynthesis to climate warming are far from clear, especially in natural ecosystems.

The acclimation of foliar respiration to warmer T_{growth} has been found in numerous studies [8,13–17], which may also be associated with plant developmental stage and other abiotic factors, such as drought and nutrient availability [18–21]. Thermal acclimation of respiration might occur via changes in the temperature sensitivity, Q_{10} , or the basal respiration, R_{10} (respiration at a reference temperature, such as 10°C) [11]. Altered Q_{10} partially reflects temperature-mediated changes in energy demand and/or available substrates [1,17,20] whereas changes in R_{10} may be associated with temperature-mediated changes in respiratory capacity, reflecting changes in mitochondrial abundance, structure and/or protein composition [22–24]. As a result, thermal acclimation of respiration may enhance plant net carbon assimilation by reducing carbon loss under warmer T_{growth} while maintaining basal rates of respiration in colder T_{growth} for subsequent recovery [12,20,25,26].

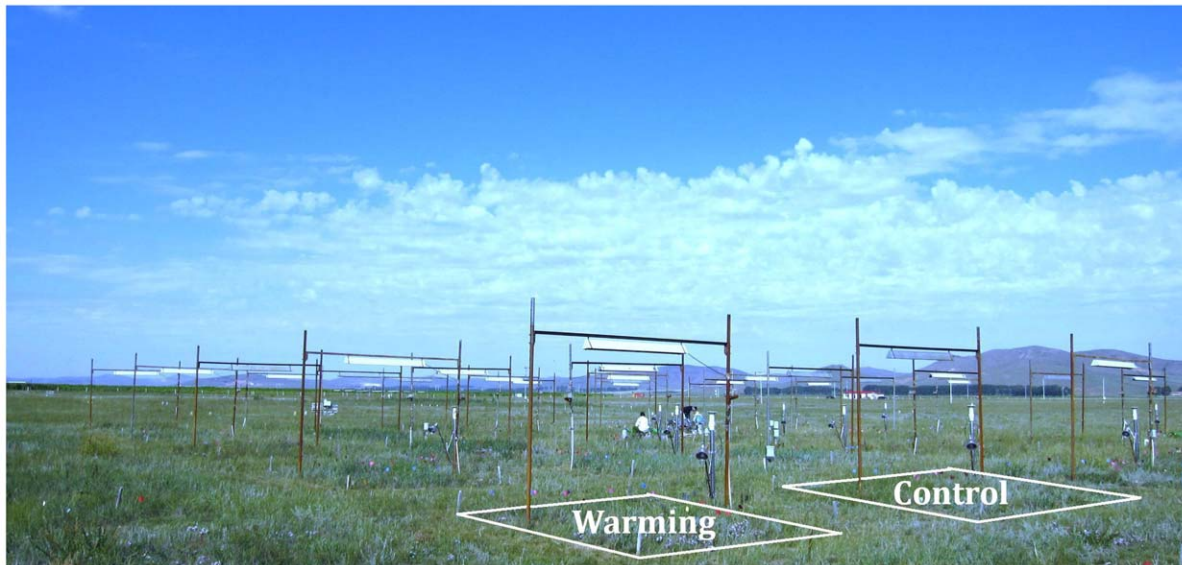


Figure 1. Layout of the experiment plots in a temperate steppe in northern China. Infrared heaters were suspended as the heating sources at the warming plots while 'dummy' heaters were suspended to simulate shading effects of the infrared heater at the control plots. doi:10.1371/journal.pone.0056482.g001

The thermal acclimation of the foliar net CO₂ assimilation rate (A_n) may involve three primary sets of processes that control the A_n/T_{leaf} curves (response of A_n versus T_{leaf}), namely respiratory, biochemical and stomatal processes [27]. First, A_n is the difference between gross CO₂ assimilation rate (A_g) and foliar dark respiration (R_d), $A_n = A_g - R_d$, which requires the decoupling of the two processes because A_g and R_d feature different thermal dynamic properties and thus involve different thermal acclimation processes [28]. This could result in a shift in T_{opt} and a change in the shape of the A_n/T_{leaf} curve. Therefore, R_d must be evaluated separately and factored out to understand the acclimation mechanisms of A_g in response to global warming [3,18,29]. Second, the acclimation of A_g to warmer T_{growth} deals with the changes in Rubisco activity [29–33] and electronic transport processes [34] where T_{growth} affects the thermal dependence of various enzymes in the dark and light reactions [35,36]. Therefore, the temperature sensitivity of the maximum rate of Rubisco carboxylation (V_{cmax}) and the maximum rate of photosynthetic electron transport (J_{max}) are associated with the acclimation of A_g [36,37]. In addition, the change in the balance between carboxylation and regeneration of RuBP, indicated by $J_{\text{max}}/V_{\text{cmax}}$ ratio, may also result in the shift of T_{opt} of A_g due to nitrogen (N) partitioning in the photosynthetic apparatus [3,31,38,39]. Finally, the temperature-dependent diffusion processes of CO₂ to chloroplasts, such as stomatal conductance (g_s) and mesophyll conductance (g_m), can also affect the thermal acclimation of photosynthesis [36,40]. Kirschbaum and Farquhar [41] showed that higher conductance could cause an increase of CO₂ concentrations in the carboxylation site (C_c) and then resulted in a shift in limitation of A_g from Rubisco to electron transport capacity. Since T_{opt} of electron transport-limited A_g is higher than that of Rubisco-limited A_g , T_{opt} of A_g was increased (0.05°C per 1 $\mu\text{mol mol}^{-1}$ CO₂) [36].

Stipa krylovii Roshev. is a keystone species in the temperate steppe in northern China [42,43]. Climate models predict this region will be 4°C warmer by 2100, which may have severe impacts on *Stipa krylovii* Roshev. [44]. Examining the respiration and photosynthesis of this species is critical to the steppe productivity and the carbon cycle of the ecosystem. The objectives

of the current study are to examine: (1) the acclimation capacity of respiration and photosynthesis to experimental warming under field conditions, and (2) the homeostasis of respiration/photosynthesis ratio in response to experimental warming in the steppe ecosystem.

Materials and Methods

Site Description

The research site (42°02' N, 116°17' E, 1324 m a.s.l.) is a typical temperate steppe located in Duolun County, Inner Mongolia Autonomous Region, China. The experiment has received the permits for the field study from the land owner, Institution of Botany, Chinese Academy of Sciences. The mean

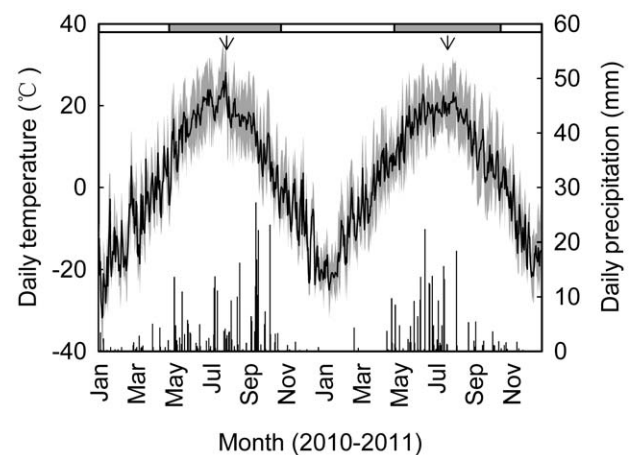


Figure 2. Daily maximum, minimum and mean air temperature (lines) and precipitation (bars) at the study site in 2010 and 2011. The filled rectangles on the top of figure indicate the growing season (May to October) and the open rectangles for the non-growing season (November to April). The arrows mark the timing of field campaigns when the gas exchange measurements were initiated. doi:10.1371/journal.pone.0056482.g002

annual temperature (MAT) is 2.1°C, with monthly mean temperature ranging from -17.5°C in January to 18.9°C in July. The mean annual precipitation (MAP) is approximately 385 mm with approximately 85% falling from May to September. The soils are chestnut (Chinese classification system) or Haplic Calcisols (FAO classification system), with 62.8% sand, 20.3% silt, and 17.0% clay respectively. The soils are characterized as sandy, slightly alkaline and nutrient poor with pH values around 7.7 and bulk density of 1.3 g cm⁻³ and soil total organic C and N concentrations of 16.1 and 1.5 g kg⁻¹ respectively. The plant communities in the temperate steppe are dominated by *Stipa krylovii* Roshev., *Artemisia frigid* Willd., *Potentilla acaulis* L., *Cleistogenes squarrosa* (Trin.) Keng., *Allium bidentatum* Fisch. ex Prokh., and *Agropyroncristatum* (L.) Gaertn.

Warming Experiment

The warming experiment was initiated in April 2006 with infrared heaters (MSR-2420, Kalglo Electronics Inc., USA; radiation output is approximately 1600 W) as the heating source (Fig. 1). Briefly, an infrared heater of 1.65 m in length was suspended at 2.25 m above the ground in each warming plot which features a dimension of 3×4 m. A reflector associated with the heater can be adjusted so as to generate an evenly distributed radiant input to the plant canopy. In the control plots, a ‘dummy’ heater with the same shape and size was suspended at the same height to simulate shading effects of the infrared radiator. The effects of warming on T_{leaf} were measured using a portable infrared thermometer (FLUKE 574, Fluke Inc., USA). The mean daytime T_{leaf} in the warming plots was increased by 2.07°C compared to the control plots. The warming experiment was designed for long-term simulation of global change and it featured a complete random block design with multiple treatments (day warming, night warming, diel warming, and N addition) and six replicates. We took advantage of this multi-factor experiment by selecting the diel warming and control plots with all the other factors kept at control levels. The details of the experiment can be found in Wan *et al.* [44] and Xia *et al.* [45].

Gas Exchange Measurements

We measured foliar gas exchange using a portable photosynthesis system (LI-6400, LI-COR Inc., USA) in the middle of the

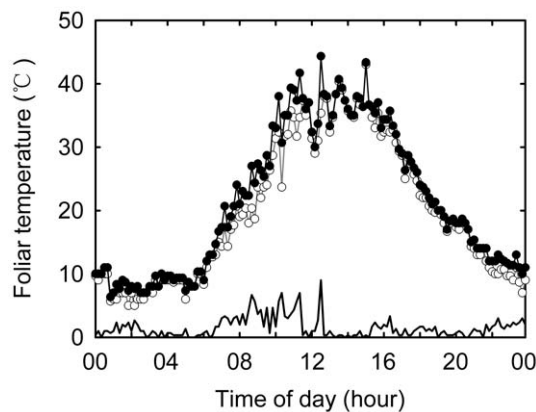


Figure 3. Representative 24-h foliar temperature (T_{leaf}) profiles from *Stipa krylovii* Roshev. grown in the control (open) and warming (filled) plots during the field measurement campaigns. Thick solid line indicates warming-induced changes in T_{leaf} between control and warming plots.
doi:10.1371/journal.pone.0056482.g003

growing seasons (late July to early August) in 2010 and 2011 (Fig. 2) to remove the effect of seasonal changes in photosynthetic and respiratory acclimation in *Stipa krylovii* Roshev. [19]. Four individuals (one individual per plot) were measured in each treatment. Eight days were required to complete all field measurements each year. Light, T_{leaf} , humidity, and CO₂

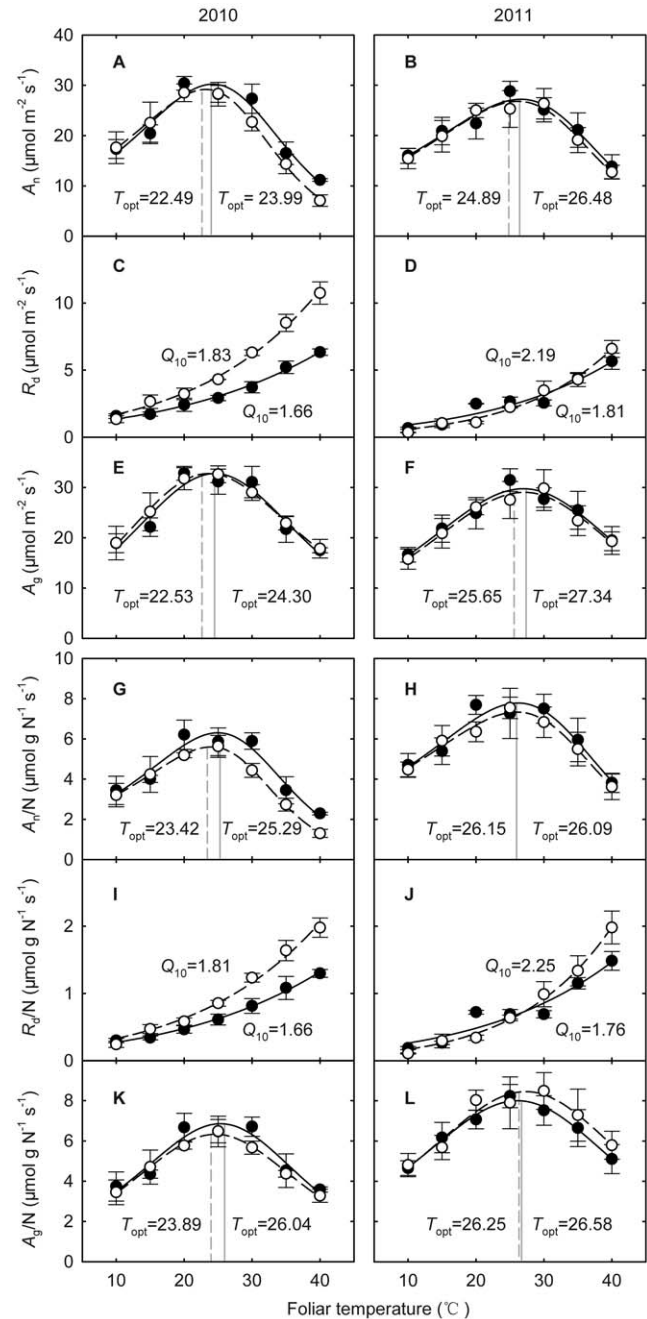


Figure 4. Warming effects on the responses of photosynthesis and respiration to foliar temperature (T_{leaf}) in 2010 (left panels) and 2011 (right panels). The filled circles indicate the warming plots and the open circles for the control plots. (A) to (F) foliar area based: (A) and (B) net CO₂ assimilation (A_n); (C) and (D) dark respiration (R_d); (E) and (F) gross CO₂ assimilation (A_g); (G) to (L) foliar nitrogen based: (G) and (H) A_n ; (I) and (J) R_d ; (K) and (L) A_g . Each data point is the average of 4 replicates.
doi:10.1371/journal.pone.0056482.g004

Table 1. Results (*P*-values) of one-way ANOVA on the effects of warming on the responses of A_n (the net CO₂ assimilation rate), R_d (dark respiration), A_g (the gross CO₂ assimilation rate), V_{cmax} (the maximum rate of Rubisco carboxylation) and J_{max} (the maximum rate of photosynthetic electron transport) expressed per unit foliar area and nitrogen to instantaneous change (10–40°C within a 5 h period) in T_{leaf} (foliar temperature) in 2010 and 2011.

Year	Parameters	<i>c</i>	ΔH_a	ΔH_d	ΔS	T_{opt}	Q_{10}	ref_{10}
2010	A_n	0.836	0.844	0.735	0.727	0.310	/	0.816
	R_d	0.027	0.046	/	/	/	0.049	0.090
	A_g	0.292	0.300	0.979	0.913	0.328	/	0.839
	V_{cmax}	0.055	0.064	/	/	/	0.062	0.784
	J_{max}	0.879	0.842	0.757	0.772	0.520	/	0.181
	A_n/N	0.726	0.732	0.575	0.612	0.323	/	0.955
	R_d/N	0.071	0.095	/	/	/	0.094	0.094
	A_g/N	0.977	0.976	0.138	0.178	0.302	/	0.996
	V_{cmax}/N	0.150	0.158	/	/	/	0.142	0.546
	J_{max}/N	0.474	0.468	0.678	0.646	0.874	/	0.381
2011	A_n	0.474	0.472	0.986	0.923	0.619	/	0.865
	R_d	0.042	0.040	/	/	/	0.042	0.050
	A_g	0.403	0.400	0.600	0.529	0.637	/	0.758
	V_{cmax}	0.723	0.712	/	/	/	0.779	0.656
	J_{max}	0.166	0.167	0.325	0.369	0.317	/	0.487
	A_n/N	0.354	0.354	0.470	0.453	0.989	/	0.886
	R_d/N	0.010	0.010	/	/	/	0.011	0.026
	A_g/N	0.306	0.305	0.604	0.554	0.933	/	0.698
	V_{cmax}/N	0.074	0.079	/	/	/	0.093	0.703
	J_{max}/N	0.463	0.468	0.215	0.223	0.115	/	0.657

c is a scaling constant, ΔH_a is the activation energy, ΔH_d is a term for deactivation, ΔS is an entropy term, T_{opt} is the thermal optimum, Q_{10} is the temperature sensitivity and ref_{10} is the estimated basal rate at the reference temperature of 10°C. Significant values (*P*<0.05) are shown bold. doi:10.1371/journal.pone.0056482.t001

concentration were independently controlled in a 2×3 cm cuvette. Given the T_{leaf} control capacity is limited (within ±6°C) with the factory setup of the LI-6400 system, we modified the T_{leaf} control system by adding metal blocks with water channels to heat or cool the peltiers, thermoelectric cooling elements. The water channels were connected to a heating/cooling water bath whose temperature was controlled by adding hot water or ice. This modification allows holding T_{leaf} at any level between 10 and 40°C during the summer growing season in the steppe.

The photosynthetically active photon flux density (PPFD) was provided by the red/blue LED light source built in the foliar cuvette calibrated against an internal photodiode (LI-6400-02B, LI-COR Inc.). The vapor pressure deficit (VPD) in the foliar cuvette was controlled by passing the air entering the cuvette through either anhydrous calcium sulfate for the lower T_{leaf} when humidity was high or bubbling air via water at higher T_{leaf} when the air was dry. CO₂ concentrations in the cuvette were controlled using an injector system (LI-6400-01, LI-COR Inc.) which functions with a CO₂ mixer and compressed CO₂ cartridges. Cuvette was sealed with plasticine to prevent leakage. Potential leakage of CO₂ out and into the empty cuvette was determined for each concentration and used to correct the measured foliar fluxes with the equations provided by von Caemmerer and Farquhar [46] and Galmés *et al.* [47]. The gas exchange system was zeroed using H₂O and CO₂ free air every day.

Typical A_n/C_i curves (A_n versus calculated intercellular CO₂ concentrations, C_i) were measured at T_{leaf} changing from 10 to 40°C with 5°C increments each. We started with the A_n/C_i curves

at low T_{leaf} (10°C) in the morning around 7:00 am finished at high T_{leaf} around noon. As to the problem of co-variance between the daily cycle and temperature, Luo *et al.* [48] and Way and Sage [3] suggested that the observed responses in the biochemical parameters resulted mainly from changes in temperature rather than changes in time of day. It usually took *c.* 5 min for T_{leaf} to reach stability at each step change in temperature. Photosynthesis was induced for 10 min in saturating PPFD (1500 μmol photons m⁻² s⁻¹) and at ambient CO₂ concentration (C_a) of 380 ppmv. Measurements were made at saturating light (1500 μmol photons m⁻² s⁻¹), and a leaf VPD between 0.5 and 2.0 kPa, except for 40°C where the VPD was 4.5±0.05 kPa. A_n was measured at cuvette CO₂ partial pressures between 50 and 1200 ppmv CO₂. The C_a was lowered stepwise from 380 to 50 ppmv and then increased again from 380 to 1200 ppmv with the total of 9 points. In total, 112 A_n/C_i curves were measured and used for the analysis of physiological parameters in this study. A_n/T_{leaf} curves (response of light-saturated A_n at 380 ppmv versus T_{leaf}) were obtained based on the A_n/C_i curves measured from 10 to 40°C.

R_d was measured by turning off the LED light source for at least 5 minutes in the cuvette after each A_n/C_i curve was accomplished [49]. All other conditions were the same as A_n/C_i curve measurements. Measurements of R_d on previously illuminated leaves were performed after a period of darkness in order to avoid light-enhanced dark respiration (LEDR) [13,18]. Five data points of R_d were logged at a 30 s interval and averaged for R_d at a given T_{leaf} . A_g was calculated by adding R_d to A_n at each T_{leaf} .

Table 2. Warming effects on the responses of A_n (the net CO₂ assimilation rate), R_d (dark respiration), A_g (the gross CO₂ assimilation rate), V_{cmax} (the maximum rate of Rubisco carboxylation) and J_{max} (the maximum rate of photosynthetic electron transport) expressed per unit foliar area and nitrogen to instantaneous change (10–40°C within a 5 h period) in T_{leaf} (foliar temperature) in the dry growing season (2010).

Parameters	Treatment	c	ΔH_a	ΔH_d	ΔS	T_{opt}	Q_{10}	ref_{10}
A_n ($\mu\text{mol m}^{-2} \text{s}^{-1}$)	Control	24.24±5.86	50.48±14.38	166.73±19.47	0.56±0.07	22.49±1.04	/	17.33±3.63
	Warming	25.73±3.69	53.96±8.92	158.17±14.21	0.53±0.04	23.99±0.87	/	16.34±1.87
R_d ($\mu\text{mol m}^{-2} \text{s}^{-1}$)	Control	20.03±0.92	45.93±2.27	/	/	/	1.83±0.05	1.70±0.12
	Warming	16.59±0.75	38.37±1.97	/	/	/	1.66±0.04	1.35±0.13
A_g ($\mu\text{mol m}^{-2} \text{s}^{-1}$)	Control	38.57±6.03	83.57±14.11	134.98±14.15	0.46±0.05	22.53±1.38	/	18.44±3.52
	Warming	29.77±4.66	63.18±11.13	135.46±9.63	0.45±0.03	24.30±0.91	/	17.59±1.88
V_{cmax} ($\mu\text{mol m}^{-2} \text{s}^{-1}$)	Control	24.68±1.26	49.08±3.08	/	/	/	1.91±0.07	46.38±2.43
	Warming	21.64±0.25	41.97±0.62	/	/	/	1.74±0.01	45.33±2.73
J_{max} ($\mu\text{mol m}^{-2} \text{s}^{-1}$)	Control	34.22±4.47	68.79±10.39	126.60±17.24	0.43±0.05	25.50±0.90	/	126.47±15.86
	Warming	35.24±4.58	71.89±10.69	132.40±4.80	0.44±0.01	26.55±1.24	/	101.15±5.31
A_n/N ($\mu\text{mol g N}^{-1} \text{s}^{-1}$)	Control	22.15±8.29	49.63±20.16	189.72±13.56	0.63±0.05	23.42±0.78	/	3.18±0.73
	Warming	27.95±13.45	63.21±32.05	201.66±14.95	0.67±0.06	25.29±1.55	/	3.13±0.58
R_d/N ($\mu\text{mol g N}^{-1} \text{s}^{-1}$)	Control	18.04±0.83	45.10±2.03	/	/	/	1.81±0.05	0.33±0.02
	Warming	15.06±1.08	38.51±2.64	/	/	/	1.66±0.06	0.28±0.02
A_g/N ($\mu\text{mol g N}^{-1} \text{s}^{-1}$)	Control	28.54±7.08	64.31±17.24	131.93±19.92	0.44±0.07	23.89±0.76	/	3.38±0.72
	Warming	29.01±13.69	65.48±32.55	176.38±16.66	0.58±0.06	26.04±1.75	/	3.39±0.60
V_{cmax}/N ($\mu\text{mol g N}^{-1} \text{s}^{-1}$)	Control	22.47±1.15	47.69±2.81	/	/	/	1.87±0.07	9.18±0.49
	Warming	19.79±1.15	41.26±2.83	/	/	/	1.72±0.06	9.68±0.61
J_{max}/N ($\mu\text{mol g N}^{-1} \text{s}^{-1}$)	Control	26.79±5.46	55.64±13.06	151.52±16.73	0.50±0.05	27.17±1.47	/	23.28±3.43
	Warming	35.83±10.49	77.39±24.84	165.48±27.26	0.55±0.09	27.58±1.98	/	19.04±2.88

c is a scaling constant, ΔH_a is the activation energy, ΔH_d is a term for deactivation, ΔS is an entropy term, T_{opt} is the thermal optimum, Q_{10} is the temperature sensitivity and ref_{10} is the estimated basal rate at the reference temperature of 10°C. Values are means (n=4, ± SE). doi:10.1371/journal.pone.0056482.t002

Estimation of V_{cmax} , J_{max} , TPU and g_m

A_n/C_c curves (A_n versus chloroplastic CO₂ concentration) were fitted to estimate V_{cmax} , J_{max} , TPU (triose-phosphate utilization) and g_m . The spreadsheet-based software of Sharkey *et al.* [50] was modified (Appendix S1) to fit the A_n/C_c curve by fixing the R_d value which was measured following the A_n/C_i curve. This modification will improve the model performance by reducing the number of estimated parameters and thus decreasing the degree of freedom in fitting the model. As in the original software the optimum of V_{cmax} , J_{max} , TPU and g_m was obtained by minimizing the root mean square error (RMSE) of each curve [51,52].

Estimation of Dependence of Reaction Rates on Temperature

The responses of R_d and V_{cmax} to T_{leaf} were fitted to a non-peaked model, following Harley *et al.* [53], due to the fact that the deactivation of R_d and V_{cmax} was not observed in our study:

$$\text{Parameter}(R_d, V_{cmax}) = e^{(c-\Delta H_a/RT_k)} \quad (1)$$

where c is a scaling constant, ΔH_a is the activation energy, R is the molar gas constant (0.008314 kJ K⁻¹ mol⁻¹) and T_k is the absolute T_{leaf} (K) [54]. Q_{10} of R_d and V_{cmax} were modeled using the following general function:

$$\text{Parameter}(R_d, V_{cmax}) = ref_{10} Q_{10}^{[(T_{leaf}-10)/10]} \quad (2)$$

where ref_{10} is the estimated basal rate at the reference temperature of 10°C, and T_{leaf} is the leaf temperature (°C). The responses of A_n , A_g and J_{max} to T_{leaf} were fitted using a peak model in view that the deactivation at high T_{leaf} was substantial:

$$\text{Parameter}(A_n, A_g, J_{max}) = \frac{e^{(c-\Delta H_a/RT_k)}}{1 + e^{[(\Delta ST_k - \Delta H_d)/RT_k]}} \quad (3)$$

where ΔH_d is a term for deactivation and ΔS is an entropy term [54,55]. The second derivative of Eqn 3 shows that T_{opt} can be calculated [56] as follows if the parameter includes a peak:

Table 3. Warming effects on the responses of A_n , R_d , A_g , V_{cmax} and J_{max} expressed per unit foliar area and nitrogen to instantaneous change (10–40°C within a 5 h period) in T_{leaf} in the wet growing season (2011).

Parameters	Treatment	c	ΔH_a	ΔH_d	ΔS	T_{opt}	Q_{10}	ref_{10}
A_n ($\mu\text{mol m}^{-2} \text{s}^{-1}$)	Control	30.91±9.71	66.17±22.71	175.99±18.90	0.59±0.06	24.89±2.47	/	15.07±2.49
	Warming	21.82±6.90	44.81±16.09	175.39±26.86	0.58±0.08	26.48±1.76	/	15.56±1.29
R_d ($\mu\text{mol m}^{-2} \text{s}^{-1}$)	Control	24.93±1.23	60.02±3.13	/	/	/	2.19±0.09	0.58±0.09
	Warming	18.95±1.97	44.85±4.88	/	/	/	1.81±0.11	0.92±0.11
A_g ($\mu\text{mol m}^{-2} \text{s}^{-1}$)	Control	39.19±13.54	85.44±31.59	167.09±24.98	0.56±0.08	25.65±2.77	/	15.27±2.45
	Warming	25.00±8.06	52.17±18.80	148.67±22.07	0.49±0.07	27.34±1.99	/	16.16±1.26
V_{cmax} ($\mu\text{mol m}^{-2} \text{s}^{-1}$)	Control	23.98±0.80	47.78±2.07	/	/	/	1.87±0.05	40.65±4.82
	Warming	23.25±1.81	45.87±4.47	/	/	/	1.83±0.11	43.85±4.84
J_{max} ($\mu\text{mol m}^{-2} \text{s}^{-1}$)	Control	27.81±5.52	54.61±13.31	167.70±27.42	0.54±0.08	31.56±1.01	/	102.85±15.77
	Warming	41.44±6.65	86.59±15.41	136.76±8.98	0.46±0.02	30.03±0.97	/	90.79±4.06
A_n/N ($\mu\text{mol g N}^{-1} \text{s}^{-1}$)	Control	28.91±9.48	64.42±22.35	277.95±128.81	0.91±0.41	26.15±3.34	/	4.38±0.71
	Warming	18.26±4.78	39.35±11.09	175.08±35.01	0.57±0.11	26.09±1.89	/	4.50±0.30
R_d/N ($\mu\text{mol g N}^{-1} \text{s}^{-1}$)	Control	24.49±1.52	62.01±3.83	/	/	/	2.25±0.11	0.16±0.03
	Warming	16.71±1.44	42.52±3.54	/	/	/	1.76±0.08	0.26±0.02
A_g/N ($\mu\text{mol g N}^{-1} \text{s}^{-1}$)	Control	37.55±11.17	84.51±26.22	193.11±55.95	0.64±0.17	26.25±3.03	/	4.37±0.64
	Warming	22.93±6.77	50.17±15.76	157.41±33.58	0.52±0.10	26.58±2.18	/	4.65±0.29
V_{cmax}/N ($\mu\text{mol g N}^{-1} \text{s}^{-1}$)	Control	23.24±0.69	48.97±1.84	/	/	/	1.90±0.05	11.67±1.37
	Warming	21.11±0.70	43.81±1.61	/	/	/	1.78±0.04	12.26±0.58
J_{max}/N ($\mu\text{mol g N}^{-1} \text{s}^{-1}$)	Control	27.40±9.59	56.67±22.90	218.93±62.97	0.71±0.20	32.46±1.55	/	28.09±3.70
	Warming	36.34±6.18	77.67±14.53	131.16±7.25	0.44±0.02	29.26±0.79	/	26.24±1.40

Values are means (n = 4, ± SE). See Table 2 for abbreviations defined. doi:10.1371/journal.pone.0056482.t003

$$T_{opt} = \frac{\Delta H_d}{\Delta S - R \ln[\Delta H_a / (\Delta H_d - \Delta H_a)]} \quad (4)$$

Estimation of Biochemical Limitations to Photosynthesis

Temperature dependence of A_g limited by RuBP carboxylation (A_c), RuBP regeneration (A_j) and TPU (A_p) were reconstructed as follows:

$$A_c = \frac{V_{cmax}(C_c - \Gamma^*)}{C_c + K_c(1 + O/K_o)} \quad (5)$$

$$A_j = \frac{J_{max}(C_c - \Gamma^*)}{4C_c + 8\Gamma^*} \quad (6)$$

$$A_p = 3TPU \quad (7)$$

where V_{cmax} , J_{max} and TPU were derived from fitted kinetic parameters (c , ΔH_a , ΔH_d and ΔS) in our study, K_c , K_o and Γ^* were derived from a general set of kinetic parameters in Sharkey *et al.* [50]. C_c was set at 250.8 ppmv in view that the mean C_c/C_a ratio

was 0.66 at ambient CO_2 concentration (380 ppmv) for all the A_n/C_i curves measured in the current study, O was the partial pressure of oxygen at Rubisco.

Foliar Characteristics

Foliar N concentration on an area basis was determined using the foliage covered in the cuvette during the gas exchange measurements. The foliage samples were first used to measure the leaf area with an area meter (Li-3100, Li-Cor Inc.) and then biomass where the samples were dried at 65°C for 48 h. Then the dry samples were ground to powder for measuring the total C and N concentrations with a CN analyzer (NA Series 2, CE Inc., Germany).

Data Analyses

The raw data from the gas exchange measurements were cleaned and processed in Excel spreadsheets where the non-linear A_n/C_c curve fitting was performed as in Sharkey *et al.* [50]. The fitting was improved by fixing R_d with the measured value (Appendix S1). Further statistical analyses were conducted using SPSS (version 17.0, SPSS Inc., USA). One-way ANOVA was used to analyze the effects of warming on (1) the foliar chemical properties (C, N, and C/N ratio) and (2) the thermal dynamic

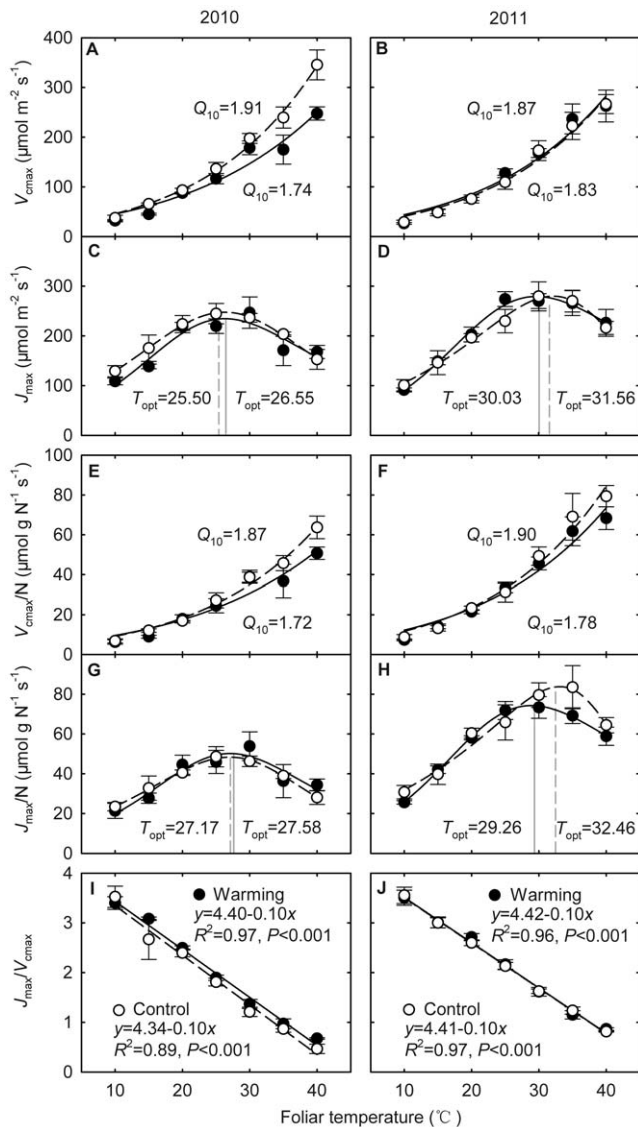


Figure 5. Warming effects on the responses of the maximum rate of Rubisco carboxylation (V_{cmax}), the maximum rate of photosynthetic electron transport (J_{max}) and the J_{max}/V_{cmax} ratio to foliar temperature (T_{leaf}) in 2010 (left panels) and 2011 (right panels). The filled circles indicate the warming plots and the open circles for the control plots. (A) and (B) area-based V_{cmax} ; (C) and (D) area-based J_{max} ; (E) and (F) N-based V_{cmax} ; (G) and (H) N-based J_{max} ; (I) and (J) the J_{max}/V_{cmax} ratio. Each data point is the average of 4 replicates.

doi:10.1371/journal.pone.0056482.g005

properties (c , ΔH_a , ΔH_d , ΔS , Q_{10} , T_{opt} and ref_{10}) of foliar gas exchange (A_n , R_d and A_g) and photosynthetic metabolism (V_{cmax} and J_{max}). Differences were considered statistically significant at $P < 0.05$. Linear regression was employed to examine relationships between foliar properties and climate (i.e. T_{growth}). T_{growth} in the control plots was an average for daytime T_{air} during the 5 d prior to gas exchange measurements in each plot. This choice was based on: (1) our observation that the bulk of individual foliar development by *Stipa krylovii* Roshev. species typically required 4–6 d; and (2) published results indicating that adjustments of foliar metabolism to climate change can occur rapidly (e.g. in a span of 1–5 d following a shift in T_{growth} [13,15,57–61]); (3) Gunderson *et al.* [60] found that T_{opt} for photosynthesis was

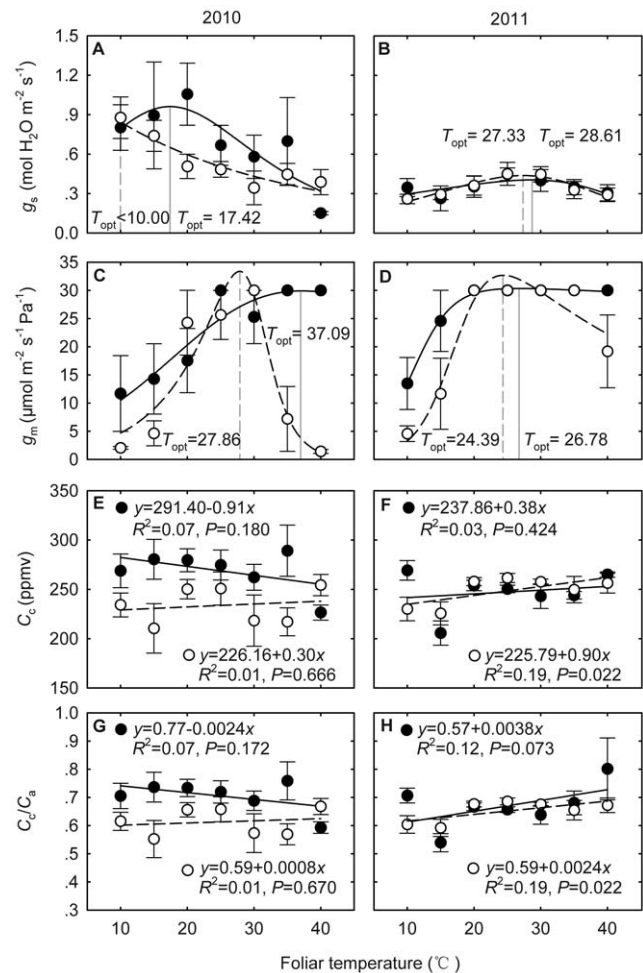


Figure 6. Warming effects on the responses of stomatal conductance (g_s) (A, B), mesophyll conductance (g_m) (C, D), carboxylation site CO_2 concentrations (C_c) (E, F), and C_c/C_s ratio (G, H) to foliar temperature (T_{leaf}) in 2010 (left panels) and 2011 (right panels). The filled circles indicate the warming plots and the open circles for the control plots. Each data point is the average of 4 replicates. **Note:** g_m is constrained to be $30 (\mu mol m^{-2} s^{-1} Pa^{-1})$ or less.

doi:10.1371/journal.pone.0056482.g006

Table 4. Foliar characteristics of *Stipa krylovii* Roshev. grown in the control and warming plots.

Year	Treatment	N concentration	C concentration	C/N ratio
2010	Control	5.34±0.07	86.66±1.48	16.22±0.16
	Warming	5.02±0.16	92.91±3.42	18.48±0.26
	P value	0.063	0.100	<0.001
2011	Control	3.41±0.05	78.12±1.35	22.92±0.15
	Warming	3.68±0.06	79.70±1.44	21.65±0.11
	P value	0.002	0.426	<0.001

Warming effects on foliar nitrogen concentrations ($g N m^{-2}$), carbon concentrations ($g C m^{-2}$) and C/N ratio ($g g^{-1}$) were analyzed using one-way ANOVA for each year. Significant values ($P < 0.05$) are shown bold (Mean ± SE, N = 28).

doi:10.1371/journal.pone.0056482.t004

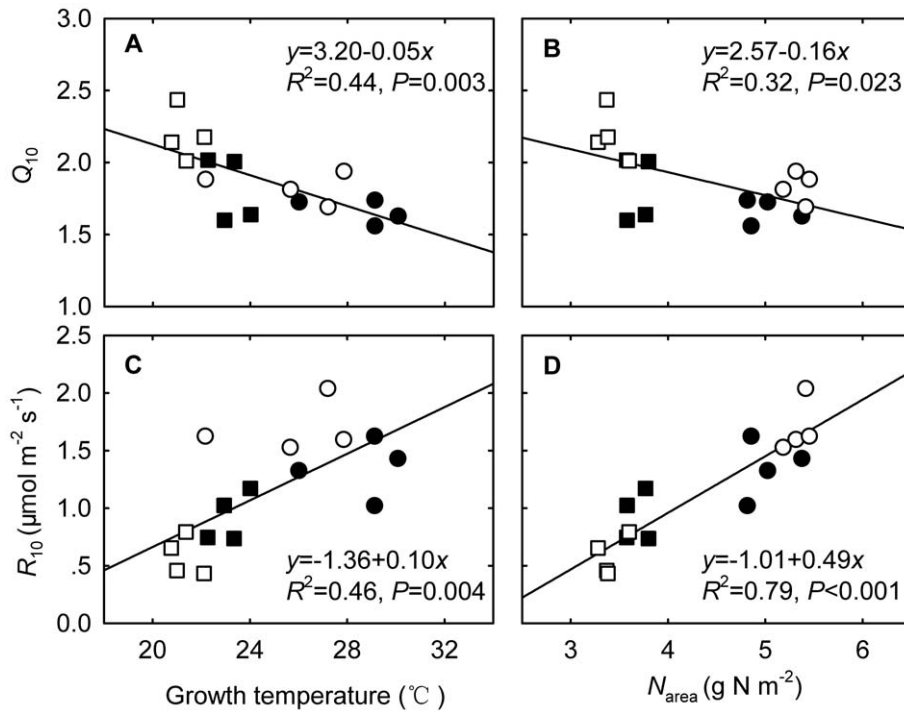


Figure 7. Responses of Q_{10} (the temperature sensitivity) (top panel) and R_{10} (the estimated basal respiration rate at the reference temperature of 10°C) (lower panel) in the control (open) and warming (filled) plots in 2010 (circles) and 2011 (squares) to T_{growth} (left panel) and foliar nitrogen concentrations (right panel), respectively. Values are means ($n=4$, \pm SE). doi:10.1371/journal.pone.0056482.g007

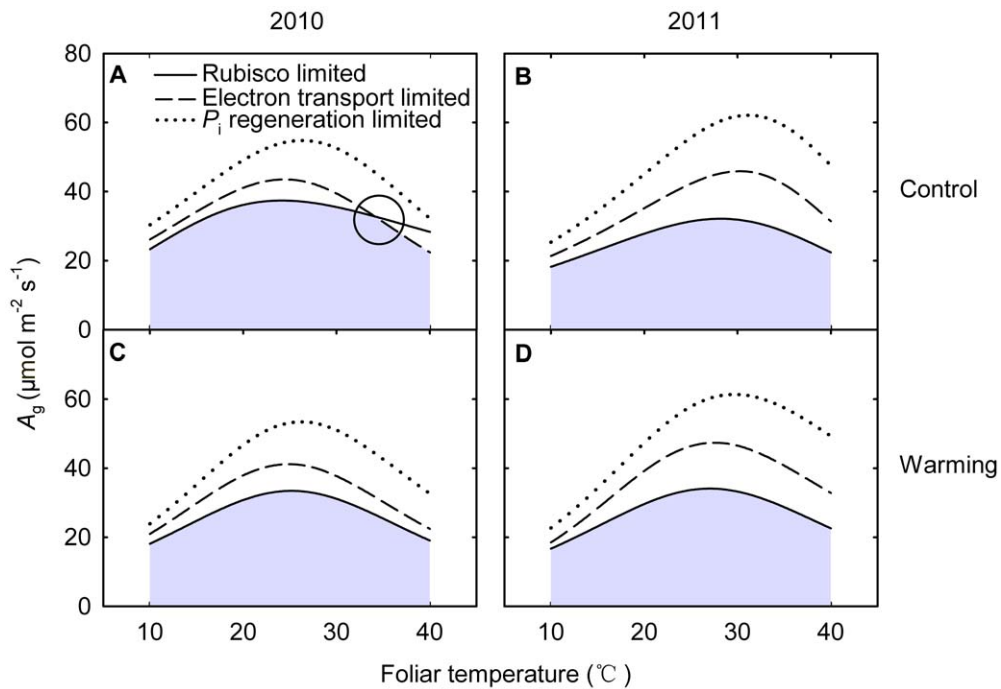


Figure 8. Warming effects on the responses of biochemical limitations in gross CO_2 assimilation (A_g) to foliar temperature (T_{leaf}) at chloroplast partial pressure of CO_2 (C_c) of 250.8 ppmv in 2010 (left panels) and 2011 (right panels). The top panels indicate the control plots and the lower panels for the warming plots. C_c was set at 250.8 ppmv considering that the mean C_c/C_a ratio was 0.66 at ambient CO_2 concentration (380 ppmv) for all the A_n/C_i curves measured. The response of A_g is delineated by the minimum value of either Rubisco-limited (solid curve), ribulose biphosphate (RuBP) regeneration-limited (dashed curve) and P_i regeneration-limited (dotted curve). Circle indicates co-limited point, moving from the Rubisco-limited state to RuBP regeneration-limited state. doi:10.1371/journal.pone.0056482.g008

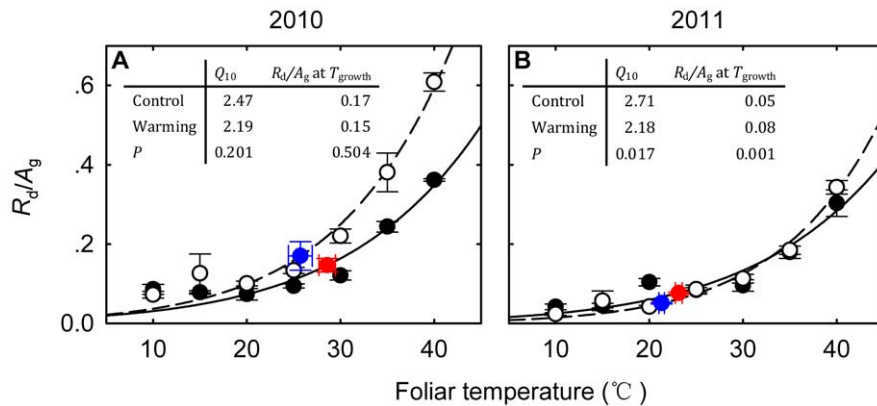


Figure 9. Warming effects on the response of R_d/A_g ratio (balance between dark respiration and gross CO_2 assimilation) to instantaneous change (10–40°C within a 5 h period) in T_{leaf} (foliar temperature) in the dry growing season (2010) (A) and the wet growing season (2011) (B). The filled circles indicate the warming plots and the open circles for the control plots. The blue and red circles indicate R_d/A_g ratio at growth temperature (T_{growth}), computed using the thermal dynamic properties (individual ΔH_a and c values for each plot) and the T_{growth} .
doi:10.1371/journal.pone.0056482.g009

strongly correlated with mean daytime T_{air} . In addition, T_{growth} in the warming plots were approximately calculated by adding warming effects (2.07°C) to the mean daytime T_{air} during the 5 d prior to gas exchange measurements in each plot.

Results

Microclimate and Experimental Warming

The meteorological data collected at the experimental site showed that the growing season of 2010 was dry while the growing season of 2011 was wet (Fig. 2). The daily mean T_{air} between 1 May, the onset of plant growth, and the time of the field measurements (27 July in 2010 and 2011) was 17.2°C in 2010 and 15.6°C in 2011 with the long-term average (1953–2011) of 15.5°C during the same period. Meanwhile, the precipitation during the same period was only 115 mm in 2010 and 183 mm in 2011 with the long-term average of 177 mm. The growing season precipitation in 2010 was only about 65% of that in a normal year, confirming 2010 was a dry year (Fig. 2).

The experimental warming significantly increased daytime T_{leaf} by 2.07°C ($P < 0.001$), on average (Fig. 3). Warming increased daytime T_{growth} in the warming plots reaching 28.59 and 23.14°C in 2010 and 2011, respectively. Meanwhile, the daytime T_{growth} in the control plots was only 25.72 and 21.31°C in 2010 and 2011, respectively. The details of the warming effects on microclimate at the study site can be found in Wan *et al.* [44] and Xia *et al.* [45].

Respiration

Warming significantly decreased respiratory temperature sensitivity, Q_{10} , in both years (both $P < 0.05$) (Fig. 4, Table 1). Q_{10} of R_d on a foliar area basis decreased from 1.83 in the control plots to 1.66 in the warming plots in 2010 ($P = 0.049$) (Table 2) and from 2.19 to 1.81 in 2011 ($P = 0.042$) (Table 3). Meanwhile, Q_{10} of R_d on a foliar N basis marginally decreased from 1.81 to 1.66 in 2010 ($P = 0.094$) and significantly decreased from 2.25 to 1.76 in 2011 ($P = 0.011$) (Table 2, 3). Warming marginally reduced base respiration rate at 10°C (R_{10}) on a foliar area basis from 1.70 to 1.35 $\mu\text{mol m}^{-2} \text{s}^{-1}$ in 2010 ($P = 0.090$) but increased that from 0.58 to 0.92 $\mu\text{mol m}^{-2} \text{s}^{-1}$ in 2011 ($P = 0.050$) (Table 2, 3). Warming effects on the R_{10} on a foliar N basis were similar to the area-based R_d (Fig. 4).

Photosynthesis

The A_n/T_{leaf} curves were typically bell-shaped in both warming and control plots (Fig. 4). Warming had little effect on T_{opt} of A_n in both years (both $P > 0.05$) (Table 1). T_{opt} of A_n on a foliar area basis was 22.49 and 23.99°C for the control and the warming plots respectively in 2010, and 24.89 and 26.48°C respectively in 2011 (Fig. 4). T_{opt} of A_g on a foliar area basis was 22.53 and 24.30°C for the control and the warming plots respectively in 2010 ($P = 0.328$), and 25.65 and 27.34°C respectively in 2011 ($P = 0.637$) (Fig. 4). Warming also had little effects on T_{opt} of A_n and A_g on a foliar N basis in either 2010 or 2011 (all $P > 0.05$) (Table 1).

Biochemical Limitations to Photosynthesis

The effects of warming on Q_{10} of V_{cmax} were not statistically significant between the warming and the control plots in both years (both $P > 0.05$) (Table 1), but we found a general decreasing trend from the control to warming plots (Fig. 5). Q_{10} of V_{cmax} on a foliar area basis was 1.91 and 1.74 for the control and the warming plots respectively in 2010 ($P = 0.062$), and 1.87 and 1.83 respectively in 2011 ($P = 0.779$) (Fig. 5, Table 2, 3). Q_{10} of V_{cmax} on a foliar N basis was 1.87 and 1.72 for the control and the warming plots respectively in 2010 ($P = 0.174$), and 1.90 and 1.78 respectively in 2011 ($P = 0.668$) (Fig. 5, Table 2, 3). The warming effects on Q_{10} of J_{max} were not detected in 2010 or 2011 (both $P > 0.05$) (Table 1). In addition, the warming effects on the slope and y -intercept of the temperature-response curves for J_{max}/V_{cmax} ratio were not statistically significant (all $P > 0.05$), though the ratio decreased linearly with the T_{leaf} (Fig. 5).

Diffusion Limitations to Photosynthesis

In 2010, a dry year, g_s in the warming plots was marginally greater than that in the control plots ($P = 0.137$), and T_{opt} for g_s was about 17.42°C in the warming plots and less than 10°C in the control plots (Fig. 6). The g_m in the warming plots was significantly greater than that in the control plots ($P < 0.001$), and T_{opt} for g_m appeared at 37.09°C in the warming plots and 27.86°C in the control plots (Fig. 6). C_c in the warming plots was approximately 35 ppmv greater than that in the control plots ($P < 0.001$), but C_c was independent of T_{leaf} in both the warming and the control plots (both $P > 0.05$) (Fig. 6). Similarly, C_c/C_a ratio was constant and

independent of T_{leaf} in the warming and the control plots (both $P > 0.05$) (Fig. 6). However, experimental warming significantly increased C_c/C_a ratio in 2010 ($P = 0.001$) with an average value of 0.70 in the warming plots and 0.61 in the control plots (Fig. 6).

In 2011, a wet year, Warming had little effect on g_s and g_m (both $P > 0.05$), which resulted in no difference in C_c between the warming and the control plots ($P = 0.860$) (Fig. 6). Experimental warming also had little effect on C_c/C_a ratio in 2011 ($P = 0.447$) with an average value of 0.67 in the warming plots and 0.65 in the control plots (Fig. 6).

Foliar Characteristics

Warming marginally decreased foliar N concentration in 2010 ($P = 0.063$), but significantly increased that in 2011 ($P = 0.002$) (Table 4). Warming had little effect on foliar carbon concentration in both years (both $P > 0.05$). Foliar C/N ratio was significantly higher in the warming plots than in the control plots in 2010 ($P < 0.001$) and the opposite was true in 2011 (Table 4).

Discussion

Acclimation of Respiration

R_d was sensitive to T_{leaf} with the R_d/T_{leaf} relationship following a typical exponential curve, but warming reduced the magnitude (Fig. 4, Table S1). Our results are consistent with previous studies [18,20,62] that the temperature sensitivity of R_d is negatively related to the T_{growth} (Fig. 7). According to the respiratory acclimation mechanisms proposed by Atkin and Tjoelker [11], the temperature-mediated change in Q_{10} is determined by the maximum enzyme activity and/or substrate availability [1,17,20]. Earlier results from the same warming experiment confirmed that day warming significantly reduced foliar starch concentrations (-6.1% , $P = 0.009$), suggesting the reduction in Q_{10} in the current study might be attributed to the lower substrate concentrations.

Foliar N concentrations induced by experimental warming in our study may also affect the temperature sensitivity of R_d , Q_{10} (Fig. 7). To date, few studies have examined the role of N in the change in Q_{10} . Turnbull *et al.* [63] found that Q_{10} of R_d for the trees in a temperate rainforest increased with increasing N availability along a soil chronosequence in New Zealand. However, Ow *et al.* [64] have reported that N had little or no impact on Q_{10} of R_d when saplings grown at high and low N availabilities were transferred to a different T_{growth} regime. Here, we found a negative correlation between Q_{10} of R_d and foliar N concentrations (Fig. 7). The detailed mechanisms are not clear, but the confounding effect of foliar N concentrations with other factors, such as temperature and precipitation, may have played an important role in the “apparent” Q_{10} [11,65,66].

In the current study we found that experimental warming marginally reduced base respiration rate at 10°C (R_{10}) in 2010 but increased that in 2011 (Table 2, 3). This could have been attributed to the differential responses of foliar N concentration to warming in the two hydrologically contrasting growing seasons. Warming marginally decreased foliar N concentration in the dry growing season (2010), but increased that in the wet growing season (2011) (Table 4). A growing number of studies [8,14,17], including our current study, have found that foliar N concentration was strongly related to R_{10} (Fig. 7). Therefore, we believed that foliar N concentration played an important role in the diverging responses of R_{10} to warming in both years.

Acclimation of Photosynthesis

Photosynthesis has long been known to acclimate to prevailing T_{growth} by shifting the T_{opt} [67]. For example, Gunderson *et al.* [60] have reported that a 3-year warming of $2\text{--}4^\circ\text{C}$ has resulted in a higher T_{opt} of A_n for five species of deciduous trees. In the current study we found that a 6-year warming of 2.07°C did not result in changes in T_{opt} of A_n (Fig. 4, Table S1). We also found that there were not statistically significant differences between the shift in T_{opt} of A_n and A_g in 2010 ($P = 0.896$) or 2011 ($P = 0.984$). This suggests that the instantaneous response of photosynthesis was independent of changes in R_d .

It has been proposed that the increase in the temperature sensitivity of V_{cmax} , indicated by ΔH_a of V_{cmax} , contributed to the thermal acclimation of photosynthesis to experimental warming [36,61,68]. However, in the current study we found that warming slightly decreased ΔH_a of V_{cmax} (Fig. 5, Table 1). Biochemically, the change in ΔH_a of V_{cmax} is closely related to the temperature dependence of Rubisco activity [69], Rubisco activation status [70,71], dimorphism of Rubisco [31], and the amount of Rubisco [72]. The lower ΔH_a of V_{cmax} obtained from the warming plots indicated that warming slightly decreased the temperature sensitivity of those processes.

Previous studies found that RuBP regeneration processes may play an important role in the thermal acclimation of photosynthesis [34,39,73]. The increase in the thermal stability of photosystem II, indicated by ΔH_a of J_{max} , has been shown to be related to the thermal acclimation of A_g to warming [34–36,74]. However, in the current study we found only minor response of ΔH_a of J_{max} to warming (Fig. 5, Table 1). This is also confirmed by our results that the RuBP regeneration seldom limited A_g (Fig. 8).

A number of studies have reported that the balance between the carboxylation and the regeneration of RuBP, indicated by $J_{\text{max}}/V_{\text{cmax}}$ ratio, can also affect the thermal acclimation of photosynthesis [39,75]. In our study, the experimental warming had little effect on the linear trend of $J_{\text{max}}/V_{\text{cmax}}$ ratio to T_{leaf} (Fig. 5). Nevertheless, in this study we found that $J_{\text{max}}/V_{\text{cmax}}$ ratio declined sharply and linearly with the instantaneous increase in T_{leaf} (Fig. 5). Many ecosystem models, such as Biome-BGC [76], have set $J_{\text{max}}/V_{\text{cmax}}$ ratio as a constant (2.1) which is independent of T_{leaf} . Wullschlegel [77] analyzed 164 A_n/G_i curves for 109 C_3 plant species which were measured under T_{leaf} ranging from 13 to 35°C and found the average $J_{\text{max}}/V_{\text{cmax}}$ ratio was 2.1. Others found that $J_{\text{max}}/V_{\text{cmax}}$ ratio was not a constant instead varying with T_{leaf} through a linear [51,78–80] or nonlinear relationship [81]. Our current results show that the relationship (between J_{max} and V_{cmax}) itself is highly temperature dependent, suggesting that photosynthesis models have to consider the temperature dependence of $J_{\text{max}}/V_{\text{cmax}}$ ratio.

In addition to biochemical limitations, the thermal acclimation of photosynthesis may also relate to CO_2 diffusion processes in leaves and chloroplasts, such as g_s and g_m , because changes in T_{growth} may affect CO_2 diffusivity, solubility, membrane permeability and stomatal movement [82–85]. Previous studies have found that increasing g_s and/or g_m can cause the increase of T_{opt} of A_n [36,40,41,67,86]. In the current study we found that warming increased g_m (Fig. 6) in 2010 which might contribute to the modest variation in T_{opt} of A_g in 2010. However, we found smaller increases in g_s and g_m (Fig. 6) in 2011, which may explain the weaker acclimation in 2011 (Fig. 4). The differential responses of CO_2 diffusion process to warming in the two hydrologically contrasting growing seasons could have been attributed to changes in soil moisture and N availability induced by warming [87]. It is noted that, so far, no consistent conclusions have been achieved on the warming effect on g_s and g_m . Some researchers found that

warming increased g_s [39,88–90] and g_m [91], and others found warming decreased g_s [92] and g_m [61], or no effect on g_s [93] and g_m [40]. Those various studies suggest that other factors, such as warming-induced water depletion and change in N availability, may have interacting effects on responses of CO₂ diffusion process to warming. These results call for multi-factor experiments, such as the combination of warming with water manipulation and fertilization [21], for understanding the mechanisms of thermal acclimation of photosynthesis under future global change.

Balance between Respiration and Photosynthesis

The acclimation of foliar respiration and photosynthesis is also reflected in R/A ratio which indicates the balance between carbon gain, loss and accumulation [1,2]. Our results show that the instantaneous (<5 h) warming at foliage level has non-linearly increased R_d/A_g ratio, indicating proportionally more carbon loss through R_d as T_{leaf} goes up (Fig. 9). However, the 6-year experimental warming has resulted in thermal acclimation of the grasses as evidenced by the decrease of the curvature of the response curve of R_d/A_g ratio to T_{leaf} (Fig. 9). It is important to note that though the balance between R_d and A_g was re-established through the thermal acclimation [6,8,9,18], R_d/A_g ratio was still increasing with T_{growth} in a wet year (Fig. 9). This means that, at foliage level, acclimation can only partially compensate the negative impact from the global warming.

Supporting Information

Table S1 Results (*P*-values) of two-way ANOVA on the effects of warming, year, and both interactions on the responses of A_n (the net CO₂ assimilation rate), R_d (dark

respiration), A_g (the gross CO₂ assimilation rate), V_{cmax} (the maximum rate of Rubisco carboxylation) and J_{max} (the maximum rate of photosynthetic electron transport) expressed per unit foliar area and nitrogen to instantaneous change (10–40°C within a 5 h period) in T_{leaf} (foliar temperature). c is a scaling constant, ΔH_a is the activation energy, ΔH_d is a term for deactivation, ΔS is an entropy term, T_{opt} is the thermal optimum, Q_{10} is the temperature sensitivity and ref_{10} is the estimated basal rate at the reference temperature of 10°C. Significant values ($P < 0.05$) are shown bold. (DOC)

Appendix S1 User's guide for the A/C_c curve fitting model with measured respiration, modified based on Sharkey *et al.*'s [50] Microsoft Excel spreadsheet-based software to reduce the number of fitting parameters (R_d is fixed in the model), version 1.2 (Last updated 25 July, 2012). (XLS)

Acknowledgments

We thank Jianyang Xia and Diheng Zhong for their help with the field measurements.

Author Contributions

Conceived and designed the experiments: YC MX SW. Performed the experiments: YC RS QY. Analyzed the data: YC MX QY. Contributed reagents/materials/analysis tools: BH SW. Wrote the paper: YC MX RS QY BH SW.

References

- Campbell C, Atkinson L, Zaragoza-Castells J, Lundmark M, Atkin OK, et al. (2007) Acclimation of photosynthesis and respiration is asynchronous in response to changes in temperature regardless of plant functional group. *New Phytol* 176: 375–389.
- Ow LF, Whitehead D, Walcroft AS, Turnbull MH (2010) Seasonal variation in foliar carbon exchange in *Pinus radiata* and *Populus deltoides*: respiration acclimates fully to changes in temperature but photosynthesis does not. *Global Change Biol* 16: 288–302.
- Way D, Sage R (2008) Thermal acclimation of photosynthesis in black spruce [*Picea mariana* (Mill.) B.S.P.]. *Plant Cell Environ* 31: 1250–1262.
- Luo Y (2007) Terrestrial carbon-cycle feedback to climate warming. *Annu Rev Ecol Syst* 38: 683–712.
- Tjoelker MG, Oleksyn J, Reich PB (2001). Modelling respiration of vegetation: evidence for a general temperature-dependent Q_{10} . *Global Change Biol* 7: 223–230.
- Gifford RM (1995) Whole plant respiration and photosynthesis of wheat under increased CO₂ concentration and temperature: long-term vs. short-term distinctions for modeling. *Global Change Biol* 1: 249–263.
- Gunderson CA, Norby RJ, Wullschlegel SD (2000) Acclimation of photosynthesis and respiration to simulated climatic warming in northern and southern populations of *Acer saccharum*: laboratory and field evidence. *Tree Physiol* 20: 87–96.
- Loveys BR, Atkinson LJ, Sherlock DJ, Roberts RL, Fitter AH et al. (2003) Thermal acclimation of leaf and root respiration: an investigation comparing inherently fast- and slow-growing plant species. *Global Change Biol* 9: 895–910.
- Dewar RC, Medlyn BE, McMurtrie RE (1999) Acclimation of the respiration/photosynthesis ratio to temperature: insights from a model. *Global Change Biol* 5: 615–622.
- Anderson JM, Chow WS, Park Y (1995) The grand design of photosynthesis: Acclimation of the photosynthetic apparatus to environmental cues. *Photosynth Res* 46: 129–139.
- Atkin OK, Tjoelker MG (2003) Thermal acclimation and the dynamic response of plant respiration to temperature. *Trends in Plant Sci* 8: 343–351.
- Rachmilevitch S, Lambers H, Huang B (2008) Short-term and long-term root respiratory acclimation to elevated temperatures associated with root thermotolerance for two *Agrostis* grass species. *J Exp Bot* 59: 3803–3809.
- Atkin OK, Evans JR, Ball MC, Lambers H, Pons TL (2000) Leaf respiration of snow gum in the light and dark. Interactions between temperature and irradiance. *Plant Physiol* 122: 915–923.
- Griffin KL, Turnbull M, Murthy R (2002) Canopy position affects the temperature response of leaf respiration in *Populus deltoides*. *New Phytol* 154: 609–619.
- Lee TD, Reich PB, Bolstad PV (2005) Acclimation of leaf respiration to temperature is rapid and related to specific leaf area, soluble sugars and leaf nitrogen across three temperature deciduous tree species. *Funct Ecol* 19: 640–647.
- Xu C, Griffin KL (2006) Seasonal variation in the temperature response of leaf respiration in *Quercus rubra*: foliage respiration and leaf properties. *Funct Ecol* 20: 778–789.
- Tjoelker MG, Oleksyn J, Reich PB, Zytzkowski R (2008) Coupling of respiration, nitrogen, and sugars underlies convergent temperature acclimation in *Pinus banksiana* across wide-ranging sites and populations. *Global Change Biol* 14: 782–797.
- Atkin OK, Bruhn D, Hurry VM, Tjoelker MG (2005) The hot and the cold: unraveling the variable response of plant respiration to temperature. *Funct Plant Biol* 32: 87–105.
- Zhou X, Liu X, Wallace LL, Luo Y (2007) Photosynthetic and respiratory acclimation to experimental warming for four species in a tallgrass prairie ecosystem. *J Integr Plant Biol* 49: 270–281.
- Crous KY, Zaragoza-Castells J, Löw M, Ellsworth DS, Tissue DT, et al. (2011) Seasonal acclimation of leaf respiration in *Eucalyptus saligna* trees: impacts of elevated atmospheric CO₂ conditions and summer drought. *Global Change Biol* 17: 1560–1576.
- Luo Y, Weng E (2011) Dynamic disequilibrium of the terrestrial carbon cycle under global change. *Trends Ecol Evol* 26: 96–104.
- Miroslavov EA, Kravkina IM (1991) Comparative analysis of chloroplasts and mitochondria in leaf chlorenchyma from mountain plants grown at different altitudes. *Ann Bot-London* 68: 195–200.
- Armstrong AF, Logan DC, Atkin OK (2006) On the developmental dependence of leaf respiration: responses to short- and long-term changes in growth temperature. *Am J Bot* 93: 1633–1639.
- Armstrong AF, Badger MR, Day DA, Barstow MM, Smith PMC, et al. (2008) Dynamic changes in the mitochondrial electron transport chain underpinning cold acclimation of leaf respiration. *Plant Cell Environ* 31: 1156–1169.
- Rachmilevitch S, Lambers H, Huang B (2006). Root respiratory characteristics associated with plant adaptation to high soil temperature for geothermal and turf-type *Agrostis* species. *J Exp Bot* 57: 623–631.
- Atkin OK, Macherel D (2009) The crucial role of plant mitochondria in orchestrating drought tolerance. *Ann Bot-London* 103: 581–597.

27. Lin YS, Medlyn BE, Ellsworth DS (2012). Temperature responses of leaf net photosynthesis: the role of component processes. *Tree Physiol* 32: 219–231.
28. Niu S, Luo Y, Fei S, Yuan W, Schimel D, et al. (2012) Thermal optimality of net ecosystem exchange of carbon dioxide and underlying mechanisms. *New Phytol* 194: 775–783.
29. Sage RF, Kubien DS (2007) The temperature response of C₃ and C₄ photosynthesis. *Plant Cell Environ* 30: 1086–1106.
30. Gutteridge S, Gatenby AA (1995) Rubisco synthesis, assembly, mechanism, and regulation. *Plant Cell* 7: 809–819.
31. Yamori W, Noguchi K, Terashima I (2005) Temperature acclimation of photosynthesis in spinach leaves: analyses of photosynthetic components and temperature dependencies of photosynthetic partial reactions. *Plant Cell Environ* 18: 536–547.
32. Weston DJ, Bauerle WL, Swire-Clark GA, Moore BD, Baird WV (2007) Molecular characterization of Rubisco activase from thermally contrasting genotypes of *Acer rubrum* L. (Aceraceae). *Am J Bot* 94: 926–934.
33. Yamori W, Noguchi K, Hikosaka K, Terashima I (2010) Phenotypic plasticity in photosynthetic temperature acclimation among crop species with different cold tolerances. *Plant Physiol* 152: 388–399.
34. Yamasaki T, Yamakawa T, Yamane Y, Koike H, Satoh K et al. (2002) Temperature acclimation of photosynthesis and related changes in photosystem II electron transport in winter wheat. *Plant Physiol* 128: 1087–1097.
35. Badger MR, Björkman O, Armond PA (1982) An analysis of photosynthetic response and adaptation to temperature in higher plants: temperature acclimation in the desert evergreen *Nerium oleander* L. *Plant Cell Environ* 5: 85–99.
36. Hikosaka K, Ishikawa K, Borjigidai A, Muller O, Onoda Y (2006) Temperature acclimation of photosynthesis: mechanisms involved in the changes in temperature dependence of photosynthetic rate. *J Exp Bot* 57: 291–302.
37. Sage RF, Way DA, Kubien DS (2008) Rubisco, Rubisco activase and global climate change. *J Exp Bot* 59: 1581–1595.
38. Hikosaka K (1997) Modelling optimal temperature acclimation of the photosynthetic apparatus in C₃ plants with respect to nitrogen use. *Ann Bot-London* 80: 721–730.
39. Hikosaka K, Murakami A, Hirose T (1999) Balancing carboxylation and regeneration of ribulose-1, 5-bisphosphate in leaf photosynthesis: temperature acclimation of an evergreen tree, *Quercus myrsinaefolia*. *Plant Cell Environ* 22: 841–849.
40. Yamori W, Noguchi K, Hanba YT, Terashima I (2006) Effects of internal conductance on the temperature dependence of the photosynthetic rate in spinach leaves from contrasting growth temperatures. *Plant Cell Physiol* 47: 1069–1080.
41. Kirschbaum MUF, Farquhar GD (1984) Temperature dependence of whole-leaf photosynthesis in *Eucalyptus pauciflora* Sieb Ex Spreng. *Aust J Plant Physiol* 11: 519–538.
42. Niu S, Li Z, Xia J, Han Y, Wu M et al. (2008) Climatic warming changes plant photosynthesis and its temperature dependence in a temperate steppe of northern China. *Environ Exp Bot* 63: 91–101.
43. Yan L, Chen S, Huang J, Lin G (2011) Water regulated effects of photosynthetic substrate supply on soil respiration in a semiarid steppe. *Global Change Biol* 17: 1990–2001.
44. Wan S, Xia J, Liu W, Niu S (2009) Photosynthetic overcompensation under nocturnal warming enhances grassland carbon sequestration. *Ecology* 90: 2700–2710.
45. Xia J, Niu S, Wan S (2009) Response of ecosystem carbon exchange to warming and nitrogen addition during two hydrologically contrasting growing seasons in a temperate steppe. *Global Change Biol* 15: 1544–1556.
46. von Caemmerer S, Farquhar GD (1981) Some relationships between the biochemistry of photosynthesis and the gas exchange of leaves. *Planta* 153: 376–387.
47. Galmés J, Medrano H, Flexas J (2007) Photosynthetic limitations in response to water stress and recovery in Mediterranean plants with different growth forms. *New Phytol* 175: 81–93.
48. Luo H, Ma L, Xi H, Duan W, Li S, et al. (2011) Photosynthetic responses to heat treatments at different temperatures and following recovery in grapevine (*Vitis amurensis* L.) leaves. *PLoS one* 6(8): e23033.
49. Wang X, Lewis JD, Tissue DT, Seemann JR, Griffin KL (2001) Effects of elevated atmospheric CO₂ concentration on leaf dark respiration of *Xanthium strumarium* in light and in darkness. *P Natl Acad Sci USA* 98: 2479–2484.
50. Sharkey TD, Bernacchi CJ, Farquhar GD, Singaas EL (2007) Fitting photosynthetic carbon dioxide response curves for C₃ leaves. *Plant Cell Environ* 30: 1035–1040.
51. Ethier GJ, Livingston NJ (2004) On the need to incorporate sensitivity to CO₂ transfer conductance into the Farquhar-von Caemmerer-Berry leaf photosynthesis model. *Plant Cell Environ* 27: 137–153.
52. Miao Z, Xu M, Lathrop RG, Wang Y (2009) Comparison of the A–C_v curve fitting methods in determining maximum ribulose 1,5-bisphosphate carboxylase/oxygenase carboxylation rate, potential light saturated electron transport rate and leaf dark respiration. *Plant Cell Environ* 32: 109–122.
53. Harley PC, Thomas RB, Reynolds JF, Strain BR (1992) Modelling photosynthesis of cotton grown in elevated CO₂. *Plant Cell Environ* 15: 271–282.
54. Harley PC, Tenhunen JD (1991) Modeling the photosynthetic response of C₃ leaves to environmental factors. In: *Modeling Crop Photosynthesis: from Biochemistry to Canopy* (eds K.J. Boote & R.S. Loomis), 1–16. Crop Science Society of America, Madison, WI.
55. Sharkey TD (1985) O₂-insensitive photosynthesis in C₃ plants. Its occurrence and a possible explanation. *Plant Physiol* 78: 71–75.
56. Medlyn BE, Loustau D, Delzon S (2002) Temperature response of parameters of a biochemically based model of photosynthesis. I. Seasonal changes in mature maritime pine (*Pinus pinaster* Ait.). *Plant Cell Environ* 25: 1155–1165.
57. Teskey RO, Will RE (1999) Acclimation of loblolly pine (*Pinus taeda*) seedlings to high temperatures. *Tree Physiol* 19: 519–525.
58. Bolstad PV, Reich P, Lee T (2003) Rapid temperature acclimation of leaf respiration rates in *Quercus alba* and *Quercus rubra*. *Tree Physiol* 23: 969–976.
59. Hartley IP, Armstrong AF, Murthy R, Barron-Gafford G, Ineson P, et al. (2006) The dependence of respiration on photosynthetic substrate supply and temperature: integrating leaf, soil and ecosystem measurements. *Global Change Biol* 12: 1954–1968.
60. Gunderson CA, O'hara KH, Campion CM, Walker AV, Edwards NT (2010) Thermal plasticity of photosynthesis: the role of acclimation in forest responses to a warming climate. *Global Change Biol* 16: 2272–2286.
61. Dillaway DN, Kruger EL (2010) Thermal acclimation of photosynthesis: a comparison of boreal and temperate tree species along a latitudinal transect. *Plant Cell Environ* 33: 888–899.
62. Atkin OK, Scheurwater I, Pons TL (2006) High thermal acclimation potential of both photosynthesis and respiration in two lowland *Plantago* species in contrast to an alpine congeneric. *Global Change Biol* 12: 500–515.
63. Turnbull MH, Tissue DT, Griffin KL, Richardson SJ, Peltzer DA et al. (2005) Respiration characteristics in temperate rainforest tree species differ along a long-term soil-development chronosequence. *Oecologia* 143: 271–279.
64. Ow LF, Griffin KL, Whitehead D, Walcroft AS, Turnbull MH (2008) Thermal acclimation of leaf respiration but not photosynthesis in *Populus deltoides* × *nigra*. *New Phytol* 178: 123–134.
65. Xu M, Qi Y (2001) Spatial and seasonal variations of Q₁₀ determined by soil respiration measurements at a Sierra Nevada forest. *Global Biogeochem Cy* 15: 687–696.
66. Davidson EA, Janssens IA, Luo Y (2006) On the variability of respiration in terrestrial ecosystems: moving beyond Q₁₀. *Global Change Biol* 12: 154–164.
67. Berry J, Björkman O (1980) Photosynthetic response and adaptation to temperature in higher plants. *Annu Rev Plant Physiol* 31: 491–543.
68. Warren CR (2008) Does growth temperature affect the temperature responses of photosynthesis and internal conductance to CO₂? A test with *Eucalyptus regnans*. *Tree Physiol* 28: 11–19.
69. Galmés J, Ribas-Carbó M, Medrano H, Flexas J (2011) Rubisco activity in Mediterranean species is regulated by the chloroplastic CO₂ concentration under water stress. *J Exp Bot* 62: 653–665.
70. Crafts-Brandner SJ, Salvucci ME (2000) Rubisco activase constrains the photosynthetic potential of leaves at high temperature and CO₂. *P Natl Acad Sci USA* 97: 13430–13435.
71. Cen Y, Sage RF (2005) The regulation of Rubisco activity in response to variation in temperature and atmospheric CO₂ partial pressure in sweet potato. *Plant Physiol* 139: 979–990.
72. Delatorre J, Pinto M, Cardemil L (2008) Effects of water stress and high temperature on photosynthetic rates of two species of Prosopis. *J Photoch Photobio B* 92: 67–76.
73. Mitchell RAC, Barber J (1986) Adaptation of photosynthetic electron-transport rate to growth temperature in pea. *Planta* 169: 429–436.
74. Armond PA, Schreiber U, Björkman O (1978) Photosynthetic acclimation to temperature in the desert shrub, *Larrea divaricata*. II. Light-harvesting efficiency and electron transport. *Plant Physiol* 61: 411–415.
75. Onoda Y, Hikosaka K, Hirose T (2005) The balance between RuBP carboxylation and RuBP regeneration: a mechanism underlying the interspecific variation in acclimation of photosynthesis to seasonal change in temperature. *Funct Plant Biol* 32: 903–910.
76. Thornton PE, Law BE, Gholz HL, Clark KL, Falge E, et al. (2002) Modeling and measuring the effects of disturbance history and climate on carbon and water budgets in evergreen needleleaf forests. *Agr Forest Meteorol* 113: 185–222.
77. Wullschlegel SD (1993) Biochemical limitations to carbon assimilation in C₃ plants—a retrospective analysis of the A/C_v curves from 109 species. *J Exp Bot* 44: 907–920.
78. Walcroft AS, Whitehead D, Silvester WB, Kelliher FM (1997) The response of photosynthetic model parameters to temperature and nitrogen concentration in *Pinus radiata* D. Don. *Plant Cell Environ* 20: 1328–1348.
79. Dreyer EW, Roux XL, Montpied P, Daudet FA, Masson F (2001) Temperature response of leaf photosynthetic capacity in seedlings from seven temperate tree species. *Tree Physiol* 21: 223–232.
80. Kattge J, Knorr W (2007) Temperature acclimation in a biochemical model of photosynthesis: a reanalysis of 36 species. *Plant Cell Environ* 30: 1176–1190.
81. Leuning R (2002) Temperature dependence of two parameters in a photosynthesis model. *Plant Cell Environ* 25: 1205–1210.
82. Flexas J, Bota J, Loreto F, Cornic G, Sharkey TD (2004) Diffusive and metabolic limitations to photosynthesis under drought and salinity in C₃ plants. *Plant Biology* 6: 269–279.
83. Bernacchi CJ, Portis AR, Nakano H, von Caemmerer S, Long SP (2002) Temperature response of mesophyll conductance. Implications for the

- determination of Rubisco enzyme kinetics and for limitations to photosynthesis *in vivo*. *Plant Physiol* 130: 1992–1998.
84. Flexas J, Ortuño MF, Ribas-Carbó M, Díaz-Espejo A, Florez-Sarasa ID et al. (2007) Mesophyll conductance to CO₂ in *Arabidopsis thaliana*. *New Phytol* 175: 501–511.
 85. Flexas J, Ribas-Carbó M, Díaz-Espejo A, Galmés J, Medrano H (2008) Mesophyll conductance to CO₂: current knowledge and future prospects. *Plant Cell Environ* 31: 602–621.
 86. Farquhar GD, von Caemmerer S, Berry JA (1980) A biochemical model of photosynthetic CO₂ assimilation in leaves of C₃ species. *Planta* 149: 78–90.
 87. Melillo JM, Steudler PA, Aber JD, Newkirk K, Lux H, et al. (2002) Soil warming and carbon-cycle feedbacks to the climate system. *Science* 298: 2173–2176.
 88. Ferrar PJ, Slatyer RO, Vranjic JA (1989) Photosynthetic temperature acclimation in *Eucalyptus* species from diverse habitats, and a comparison with *Nerium oleander*. *Aust J Plant Physiol* 16: 199–217.
 89. Williams DG, Black RA (1993) Phenotypic variation in contrasting temperature environments: growth and photosynthesis in *Pennisetum setaceum* from different altitudes on Hawaii. *Funct Ecol* 7: 623–633.
 90. Hikosaka K (2005). Nitrogen partitioning in the photosynthetic apparatus of *Plantago asiatica* leaves grown at different temperature and light conditions: similarities and differences between temperature and light acclimation. *Plant Cell Physiol* 46: 1283–1290.
 91. Makino A, Nakano H, Mae T (1994) Responses of ribulose-1,5-bisphosphate carboxylase, cytochrome *f*, and sucrose synthesis enzymes in rice leaves to leaf nitrogen and their relationships to photosynthesis. *Plant Physiol* 105: 173–179.
 92. Mooney HA, Björkman O, Collatz GJ (1978) Photosynthetic acclimation to temperature in the desert shrub, *Larrea divaricata*. *Plant physiol* 61: 406–410.
 93. Hendrickson L, Ball MC, Wood JT, Chow WS, Furbank RT (2004) Low temperature effects on photosynthesis and growth of grapevine. *Plant Cell Environ* 27: 795–809.